International Journal of
INTELLIGENT SYSTEMS AND APPLICATIONS IN ENGINEERING
ISSN:2147-6799 www.ijisae.org Original Research Paper

Microstructure Analysis and Mechanical Properties Studies on the Magnetic Pulse Welded AA 6061 T6 Tubular Joints

Pravin Kumar. M[1], Varahamoorthi. R[2], Sundarraj. C[3]

Submitted: 06/05/2024 **Revised:** 19/06/2024 **Accepted:** 26/06/2024

Abstract: In this investigation, AA 6061 T6 tubular joints were produced through Magnetic Pulse Welding technique. The joints were produced varying the significant process parameters Discharge Voltage, Standoff distance and Overlap length in lap mode configuration. A 100kJ capacity B-Max made MPW equipment was used to produce the joints. The electromagnetic force required to accelerate the Flyer tube towards the target rod at high speed was generated by a Single turn coil energized through capacitor banks. The microstructure and the mechanical properties of the joints were studied and evaluated. The welded specimens were prepared for tensile testing using Wire cut EDM. A maximum tensile strength of 303 MPa was observed for the parameter values of Discharge Voltage 12kV, Stand-off Distance 1.75mm and Overlap length of 8mm. The maximum tensile strength obtained is 98.05% of the actual Tensile Strength of the base metal. Compression test was done on the specimen joint with maximum tensile strength and the tests revealed that failure happened at the lighter Flyer metal which indicates sound welding strength. Microhardness survey was conducted across the base metal and the weld interface for the samples with tensile strength at high, medium and low ranges. The results revealed that the Vicker microhardness was 138 HV at the weld interface which is 1.76 times higher than the actual hardness of the base metal. Microhardness values varied from 100 HV to 120HV at the base metals. Microstructural studies showed well defined wavy, flat and discontinuous weld interface. Joint strength was based on the amplitude of the interface waves, flatter waves resulted in relatively weaker strength and high amplitude waves ensured high strength. Presence of Mg and Si in the interface enabled formation of Mg2Si precipitates resulting in high hardness.

Keywords: *Magnetic Pulse Welding (MPW), AA 6061 T6, Tensile strength, Microhardness, Discharge Voltage, Stand- off distance, Overlap length, Precipitates.*

1. Introduction

Owing to the high strength to low weight property of Aluminium alloys, they find their utility in a wide range of industrial applications. However, joining of Al alloys cannot be appropriately done using fusion welding methods. One of the prime reasons being the high thermal conductivity of Al, which will push away heat quickly during fusion welding and hence joining has to be done thick and fast. Also the formation of Al_2O_3 while welding at higher temperature will result in brittle poor joints. Laser welding of Al alloys too is difficult as the Al has high reflectivity. Solid state welding techniques like Diffusion bonding, Friction Stir welding, Explosive welding and Magnetic pulse welding can be used to join Al alloys. In comparison, Diffusion bonding is a slower process, FSW is limited to only Butt joints, explosive welding though similar in principle as MPW is highly dangerous and is best suited for larger workpieces. Among these solid state welding techniques, Magnetic Pulse Welding stands out with better advantages and is capable of producing cleaner, faster, high strength and less expensive joints.

MPW technology is applicable to tube-to-tube or tube to-bar configurations. Parts are configured to form a nominally lap-type joint. The process essentially functions by discharge of charged capacitors into an induction coil that encompasses the parts to be joined [1,3]. Magnetic pulse welding (MPW) is a high-speed, solid state welding process that has the potential to significantly reduce manufacturing costs, especially for joining tubular structures [2].

The basic equipment required for MPW process include a high power source, the capacitor, a discharge switch and a coil. A high intensity current flowing through a coil near an electrically conductive material [Fig. 1], locally produce an intense magnetic field that generates eddy currents in the flyer according to Lenz law. The induced electromotive force gives rise to a current whose magnetic field opposes the original change in magnetic flux. The effect of this secondary current moving in the primary magnetic field is the generation of a Lorentz force, which accelerates the flyer at a very high speed. If a piece of material is placed in the trajectory of the flyer, the impact will produce an atomic bond in a solid state weld [7].

[1]*Research Scholar, Annamalai University, Department of Manufacturing Engineering, Faculty of Engineering and Technology, Annamalai University, Chidambaram-608002, Tamilnadu, India, pravin@pkiet.edu.in*
[2]*Professor, Annamalai University, Department of Manufacturing Engineering, Annamalai University, Chidambaram- 608002, India.*
[3]*Professor/Principal, AVC College of Engineering, Mannampandal, Mayiladuthurai, Tamilnadu, India.*

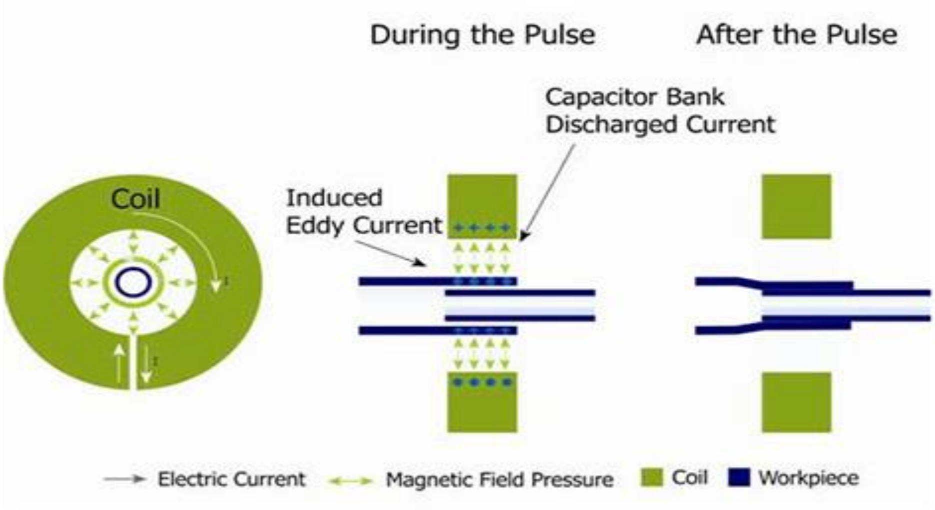

Fig. 1. Schematic Representation of MPW Process for Producing

Magnetic pulse welding has never achieved a clear place amongst mainstream manufacturing processes. Though this technique is known for a long time, there are still opportunities of development and application, especially for joining multi-materials. [6]. The precipitation hardened Aluminium 6061 T6 alloy finds its wide application in aircraft and aerospace industries, in marine fittings, in camera lenses, electrical fittings, automotive parts and alike aluminium possesses high thermal conductivity, high thermal expansion coefficient, low melting temperature making it's welding difficult than others.

It has been shown for similar metal Al/Al pairs that the wave formation characterizes an efficient interfacial bonding, which involves hardening due to a grain refinement and significantly large plastic deformation at the interface. Consequently, increasing the collision energy and thus the wave height, is recommended to improve the joint strength [13–14].

The significance of MPW technique over traditional welding techniques is that a tubular weld joint can be produced in 10microsecond and while producing aluminium joints, there is no HAZ and/or other weld defects, which are typical of conventional fusion welding processes. Moreover, for heat treated aluminum alloys, joints of very good quality can be produced with this technique. Since the initial investment is high compared to other joining techniques, MPW technique is presently used in limited application such as sheet to sheet but welding of tube to flange is rarely studied and reported [5]. In this study, Al 6061tube to rod in lap joints were produced by MPW process and their Microstructural Characteristics were studied and correlated with the mechanical properties of the base metals.

2. Experimental Procedure

2.1 Equipment Details

In the present study, joints were produced using a MPW equipment fabricated by B-Max Company [Fig 2]. Welding was performed by electromagnetic compression. The maximum energy of the system was 100kJ, maximum discharge 25kV, Maximum Discharge frequency was 60kHz. Capacitor bank of 160 µF was used to supply the required energy and Skin depth of 640 µm. Single turn coil of diameter 68 mm and thickness 30mm were used for the study [Fig. 4]. High density Polyethylene (HDPE) holders and stoppers were used for fixing of the workpieces with the coil coaxially. Single pulse was used for producing the joints.

Fig. 2. MPW Equipment

2.2 Material

Precipitation hardened aluminium alloy Al 6061 T6 was chosen as the workpiece material with Flyer metal in Tube form and the Target metal in rod form [Fig. 3 & 4]. The chemical composition of Al 6061 T6 and their mechanical properties are furnished in Table 1 and Table 2.

Table 1. Chemical Composition of Al6061 T6

% Si	% Mg	%Mn	%Fe	% Cr	% Cu	% Zn	% Ti	% V	% Zr	% Al
0.0740	0.850	0.040	0.130	0.090	0.250	0.010	0.020	0.003	0.003	0.9757

Table 2. Mechanical Properties of Al6061 T6

Tensile strength (MPa)	Yield Strength (MPa)	% Elongation	Fatigue Strength (MPa) at 500 mil cycles	Melting Point (°C)	Thermal Conductivity (W/mk)	Density (kg/m³)	Youngs Modulus (GPa)	Hardness (Vickers)	Electrical Resistivity (ohm-m)
309	276	10	97	650	209	$2.7x10^3$	70	80	4.32e-8

The Target material is in Solid form for its entire length of 200mm with diameter 63 mm which can be altered for realizing required Stand-off distance dimensions. Flyer metal measures 200mm with Outer diameter 66mm and Inner diameter 64mm. 25 mm length of the Flyer metal is in tubular form, this hollow section of the Flyer can be positioned with respect to the coil thickness to get the required dimension of Overlap length.

2.3 Welding

The range of the process parameters were selected as Discharge Voltage (V) – 12 kV to 16 kV, Stand-off distance (D) – 1.75mm to 2.5mm and Overlap lap length (L)- 7.5mm- 8mm. Experiments were conducted as per the design matrix employing Central Composite Design (CCD) using Design Expert Version 11 software. To get the Standoff distances of 1.58mm, 1.75mm, 2mm, 2.25mm and 2.42mm the Target rods were machined to diameters of 60.84mm, 60.5mm, 60mm, 59.5mm and 59.16mm respectively [Fig 3].

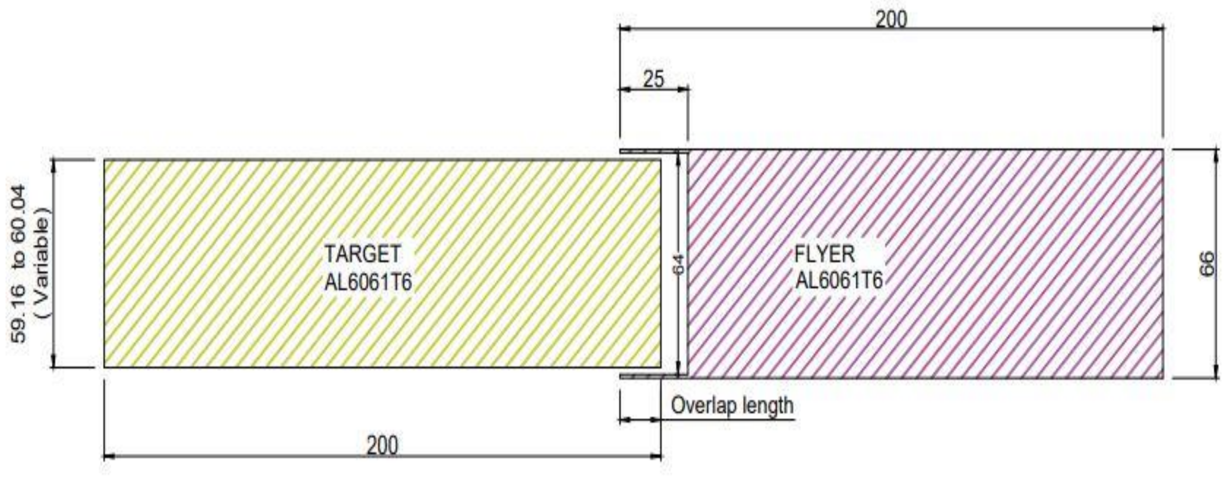

Fig. 3. Work Station Set up

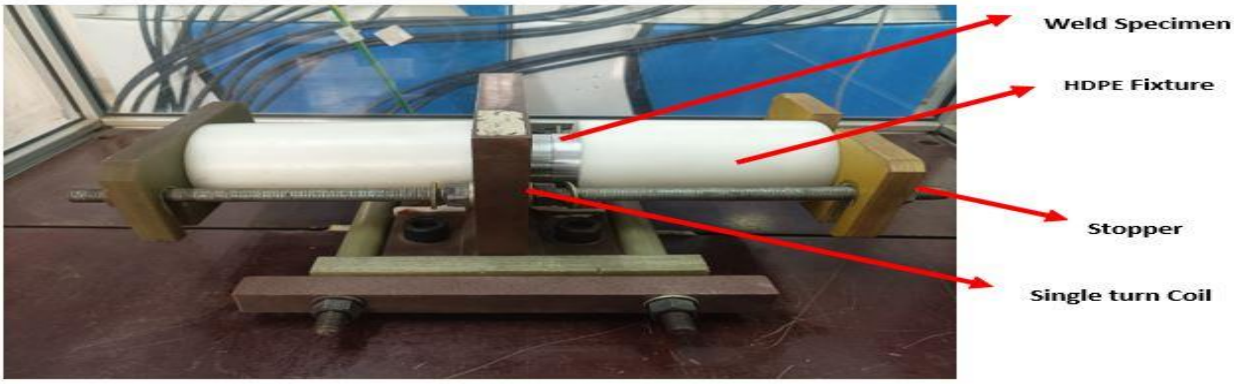

Fig. 4. Work Station Set up

Fig. 5. Specimen after weld

3. Mechanical Testing

3.1. Tensile Shear Fracture Load (TSFL)Testing

Tinius Olsen model, Universal Testing machine of 1000 N capacity, was employed for the Tensile tests. The machine has speed resolution and displacement resolution of about 0.001mm/min and about 0.0001 mm respectively. From every tensile Specimen, two samples were extracted by slicing the MPW joints using Electric Discharge Machining (EDM) as shown in the [Fig. 6 and 7]. The samples were then used to evaluate tensile strength using the Universal Tensile Testing machine. The average of the two was considered the tensile strength. The optimized set of process parameters were found and the tensile shear fracture load (TSFL) was recorded as in Table 3.

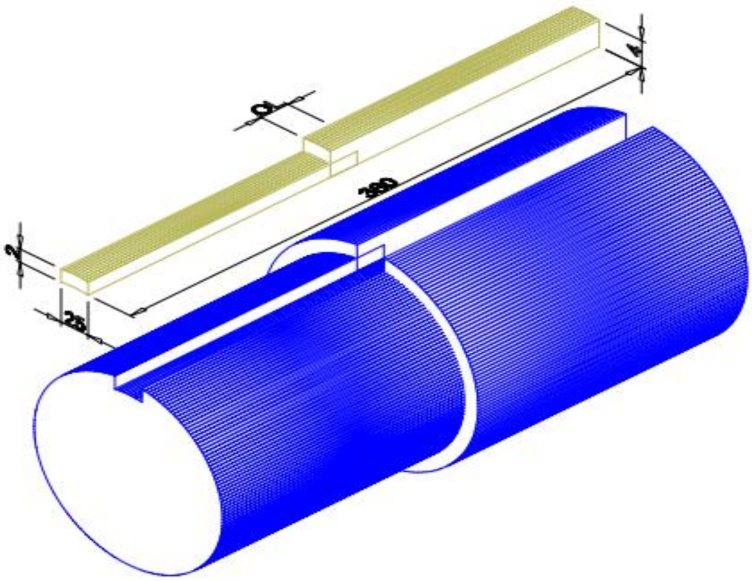

Fig. 6. Schematic Representation of Tensile Specimen

Fig. 7. Actual Tensile Specimen

Table 3. Optimized Parameters

Sl. No.	PARAMETERS	UNIT	VALUE	RESPONSE TSFL (in MPa)
1	Discharge Voltage (V)	kV	12	303
2	Stand Off Distance(D)	mm	1.75	
3	Overlap Length(L)	mm	8	

3.2. Compressive Strength Test

In order to evaluate joint strength, Compression test was performed on the MPW specimen produced for the optimum parameter values with the dimensions Flyer outer diameter 66 mm, thickness 2mm and Length 35 mm, Target diameter 60.5mm and Length 30mm as shown in Fig.8 Universal Testing machine [Fig.9] was used for the Compression test and the test was done as per the ASTM E9-09 standard.

Fig. 8. MPW Specimen

Fig. 9. Compression Test

4. Microstructural Analysis

The weld specimen produced with the process parameters as illustrated in the Table. were subjected to metallographic examination using FESEM, SEM of Zeiss make Model EVO 18. For Line scanning and Elemental mapping EDX machine of EDAX make was used. The TSFL of the specimen which ranged from 197 MPa to a maximum of 303 MPa as per the Table were chosen for the study. The study was concentrated at the weld interface, Target metal and the Flyer metal.

Table 4. TSFL of the Samples with Parameters

Sample	Process Parameters			TSFL (MPa) Experimental
	DV (kV)	**SOD (mm)**	**OL (mm)**	
M1	14	2	7.75	281
M2	14	2	7.33	269
M3	12	1.75	8	303
M4	16	1.75	7.5	243
M5	17.36	2	7.75	197
M6	16	2.25	7.5	231

The **Field Emission Scanning Electron Microscope** (FESEM) has a much brighter electron source and smaller beam size than a typical SEM increasing the useful magnification of observation and imaging up to 500000 x.

For sample preparations, specimens were cut along the center line of joints using a Wire cutting machine which would potentially avoid any microstructural changes. The samples were then drenched in phenolic to expose the center surface of joints. SiC abrasive paper was used to progressively grind all samples and polished by a polishing machine. Finally, the metallographic samples were etched for 25 s by Keller's reagent (95 mL water, 2.5 mL HNO3, 1.5 mL HCL, 1.0 mL HF). The prepared samples are illustrated in Fig.8.

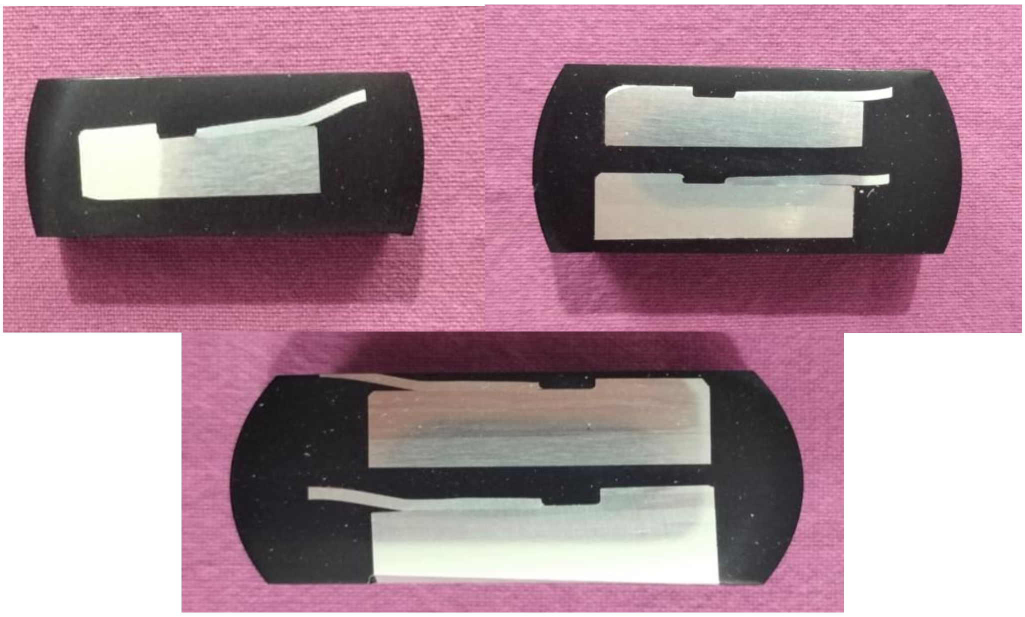

Fig. 10. Specimen for Microstructural Studies

4.1 Microhardness Survey

Microhardness testing was done using Vicker's Microhardness testing machine, Metsuzawa, Japan MMT-X7/MMS250X make with range 5gm- 1kg. All the six specimen as detailed in the Table 4 were tested for hardness at the Flyer metal, Target metal and the weld interface. A Load of 300 gm was applied for the test. Samples were prepared and testing was done as per the

ASTM E92-17 standard. The hardness values thus obtained was correlated with the Tensile strength and the microstructural characteristics of the base metals and weld interface.

5. Results and Discussions

5.1 Tensile Strength

The highest Tensile Shear Fracture Load (TSFL) was observed as 303 MPa which is 98.04% of the actual tensile strength of Al 6061 T6 as illustrated in the Table. The TSFL of the specimen varied from a minimum of 197 MPa to a maximum of 303 MPa. Failure during tensile test was observed at the weakest zone the Flyer metal [Fig 9] which authenticates sound weld quality. The varied TSFL of the specimen can be attributed to the distribution of precipitates and their sizes. Fine precipitates ensured high bonding strength.

Table 5. TSFL of the best and worst sample

Sample	Process Parameters			TSFL (MPa) Experimental	Tensile Strength of base metal Al 6061 T6 (MPa)
	DV (kV)	SOD (mm)	OL (mm)		
M3	12	1.75	8	303	309
M5	17.36	2	7.75	197	

Fig. 11. MPW Specimen after Tensile Fracture

5.2 Compressive Strength

During compressive test, it was observed that failure happened in the Flyer tubular part of Al 6061 T6 [Fig 10] which is the weakest portion of the mating metals. This is an indication of good bonding strength between the flyer and target.

As per the Load vs Displacement Plot [Fig.11], the maximum load strength was found to be 58.42 kN, the maximum displacement was 8.66mm and the maximum Compressive Strength was 0.120 kN/mm^2.

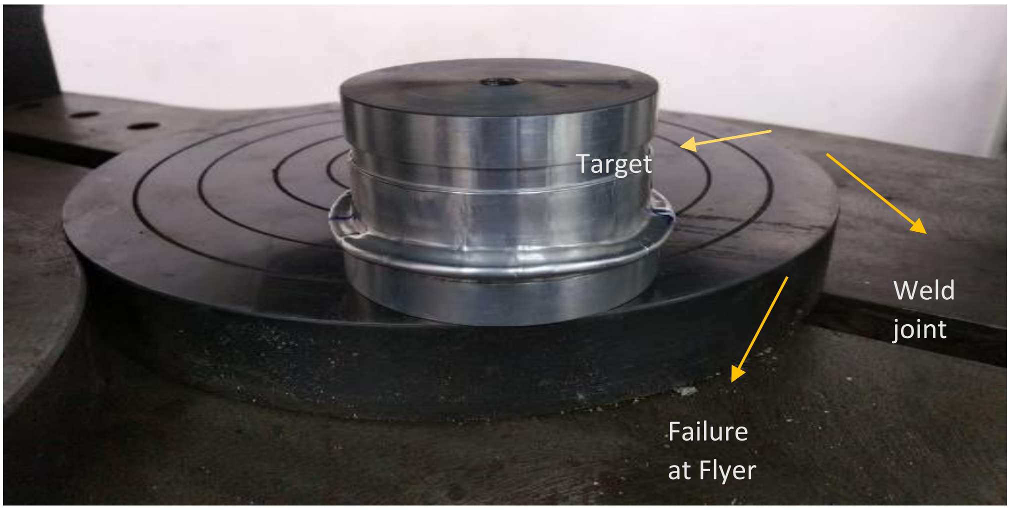

Fig. 12. Specimen after Compressive fracture

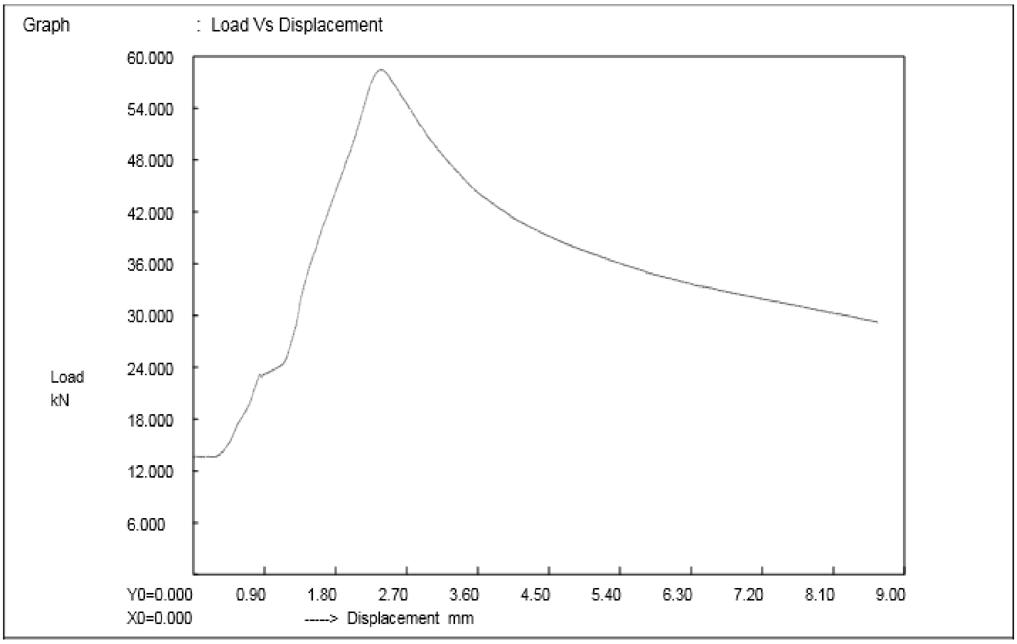

Fig. 13. Load Vs Displacement Plot

5.3 Microhardness

Microhardness survey was carried out on the weld samples at Flyer metal, Target metal and the Weld interface to evaluate the metals behavior in different zones of the weld joint. M3 was the best sample with highest tensile strength and M5 was the worst sample with lowest tensile strength.

Before the hardness survey on the weld, it is essential to measure of the hardness of the base metal AA 6061 T6 which had an average value of 80 HV. The hardness was found to be the highest at the weld interface than the base Flyer and target metals as illustrated in Table 6 and Fig.12. This can be attributed to the high rate of Strain hardening happening at the interface. It was also found that the adjacent zones of the weld interface of the base metals had hardness higher than other zones of the base metals and lower than the interface and this may be due to the strain hardening at the interface extended to the nearer zones.

It was observed that the hardness value is higher in the weld zone 138 HV than the base metal target metal and Flyer which was falling between 100 HV to 120 HV as indicated in the Fig.12.

Table 6. Hardness of the samples

Distance from the Weld (mm)	**Hardness Value of the Samples in HV 300gm**					
	M1	**M2**	**M3**	**M4**	**M5**	**M6**
-15	109	103	108	109	100	103
-10	112	106	112	111	101	103
-5	114	107	117	113	103	105
0	134	132	138	117	104	114
5	120	108	115	114	102	104
10	117	105	113	113	100	103
15	115	102	111	108	100	103

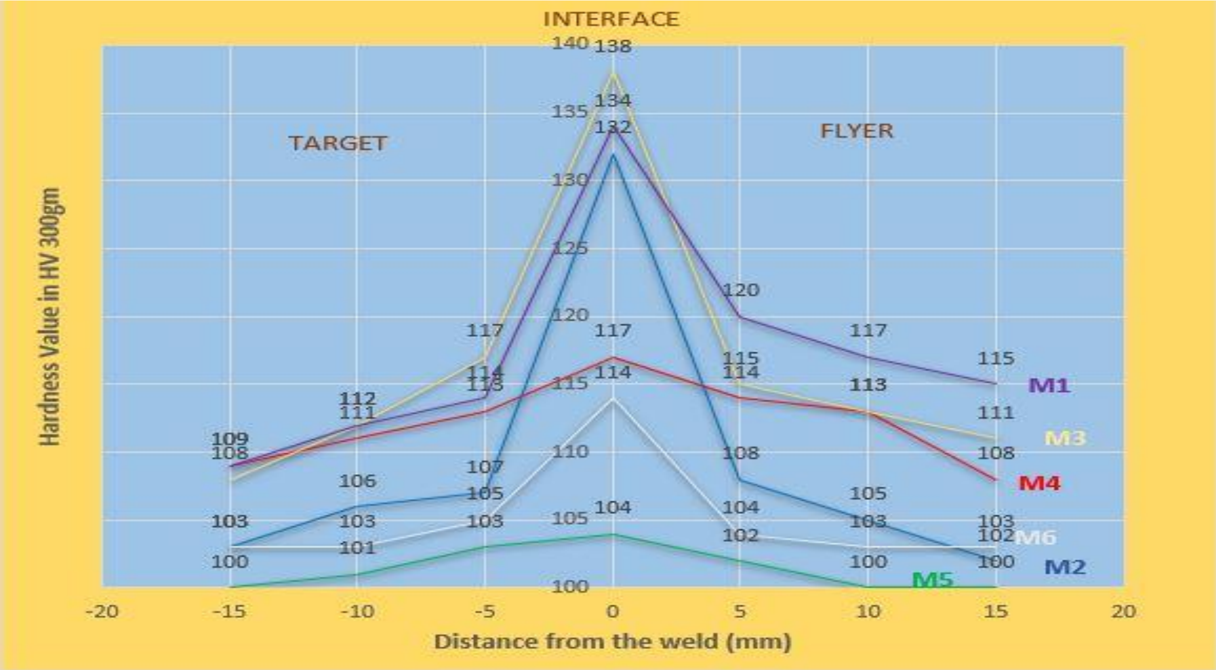

Fig. 14. Vicker's Microhardness Survey

The highest hardness of 138 HV was found in the weld interface of the Sample M3 which was welded at the optimized parameters whereas the lowest hardness of 104 HV was observed in Sample M5. It is interesting to note that the highest hardness thus measured in the interface is 1.72 times greater than that of actual hardness of the base metal and the highest hardness in the base metals of the weld sample is 1.25 times greater than that of its actual hardness.

The samples welded with Discharge voltage of 12 kV and 1.75 mm Stand-off distance exhibited better hardness and the highest Discharge Voltage of 17.33 kV and 2mm Stand-off distance exhibited lowest hardness. At Discharge Voltage of 17.33 kV, the energy dispersed on the flyer metal is very high and it is accelerated with very high velocity towards the target metal. The 2mm Stand-off distance is not sufficient for the flyer metal to reach its maximum velocity and hence the strain hardening is considerably low which resulted in low hardness. In general, the hardness values of the samples are in good agreement with their TSFL values.

5.4 Microstructural Characterization

Due to high velocity impact between the moving Flyer metal and the stationary Target metal, transfer of material happens between the mating parts and this becomes one of the reasons for increase in hardness at the interface or transition zone. For MPW joints of AA6061T6 tubes, metal continuity can be observed at the bonded interface. The wavy pattern [Fig. 13(c)] at the interface is primarily because of the discontinuities in the flow velocity. The mass flow between the materials is the result of instabilities caused at the interface due to the travel of two fluids at different velocities. The interface of a MPW joint can exhibit either a continuous wave or a Straight line pattern. Wavy pattern results in sound weld joint while the straight line pattern results in low bonding strength. Discontinuities in the wave pattern [Fig. 13(o)] will potentially produce partial joints at the circumference, this may be attributed to the differential impact velocities of the Flyer metal around the periphery of the metal.

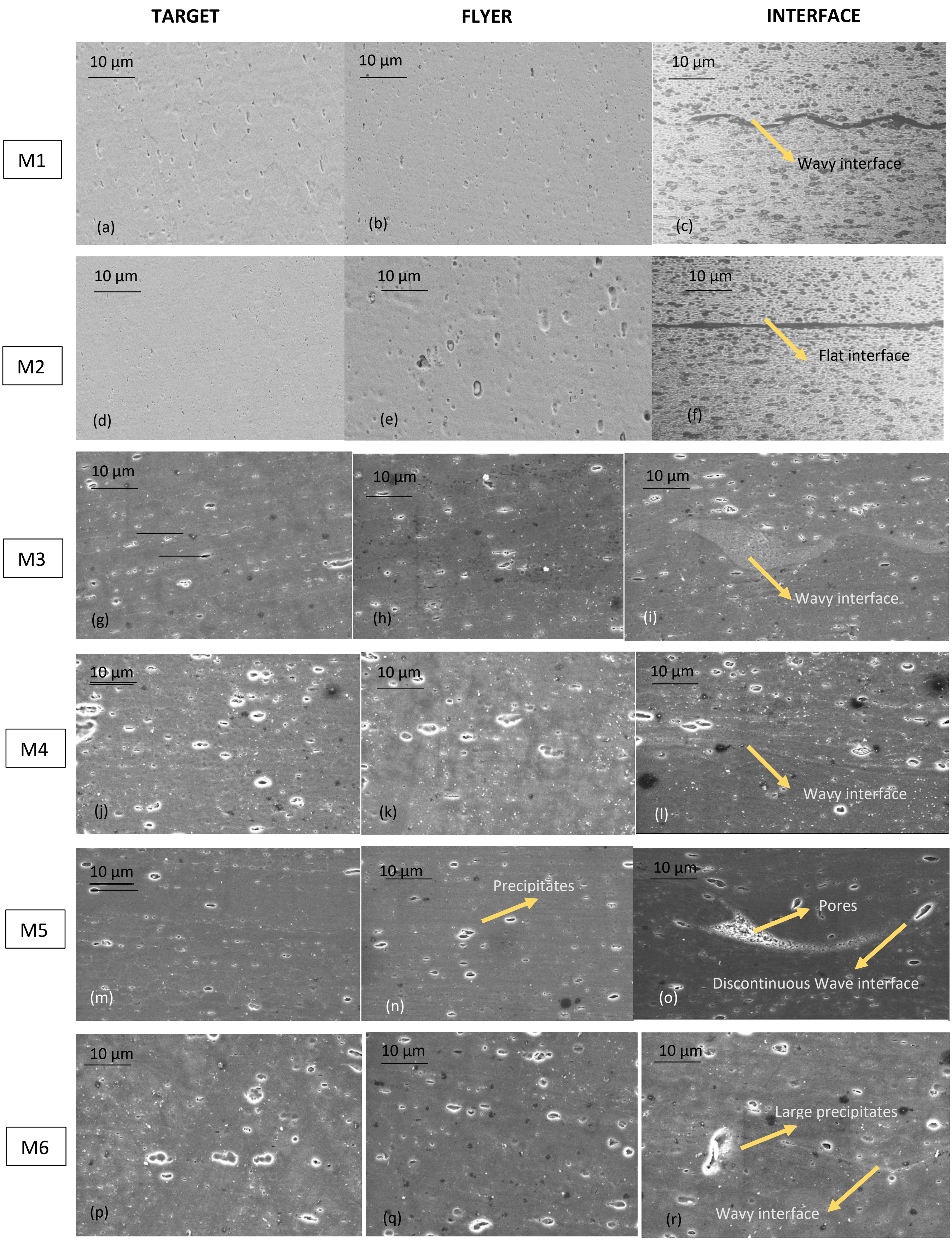

Fig. 15. SEM Pictures of 6 specimens

Since the base metals are similar, there is very little difference in the distribution of Mg_2Si precipitates as shown in the Fig 13(a,b,d,e,g,h,j,k,m,n.p,q). However, SEM images of the interface show different patterns. Fig 13 (c,f,i,l,o,r). SEM images of sample M3, M1 and M4 have interfaces with well-defined Wave pattern which promotes better interlocking of the base metals. Fig. show uniform distribution of fine precipitates in the interface resulting in increase in hardness. Waves with similar wavelength and amplitude throughout the interface result in the strongest joint as depicted by Fig 13(c)(,i) Sample M3. SEM image of Sample M2 Fig.13(f) exhibits a straight line interface which is the reason for the reduced tensile strength and hardness. Reduced hardness at the interface of sample M5 can be attributed to the discontinuous wave pattern and the presence of larger precipitates which hinder strain hardening. Sample M5 Fig.13(o) also exhibits porous welding interface which is potentially facilitated pores nucleation, coalescence and growth in sequential order within the molten intermediate phase and this is very important contributor of reduced hardness in the interface.

Three different zones exist in a MPW tubular weld joint, Run in, Weld and Run out zones as depicted in the Fig 14. Metal joining occur at the middle part and Run in and Run out zones occur on either side. Deformation of Target tube declines gradually from the Run in zone to the Run out zone and weld zone show appreciable deformation.

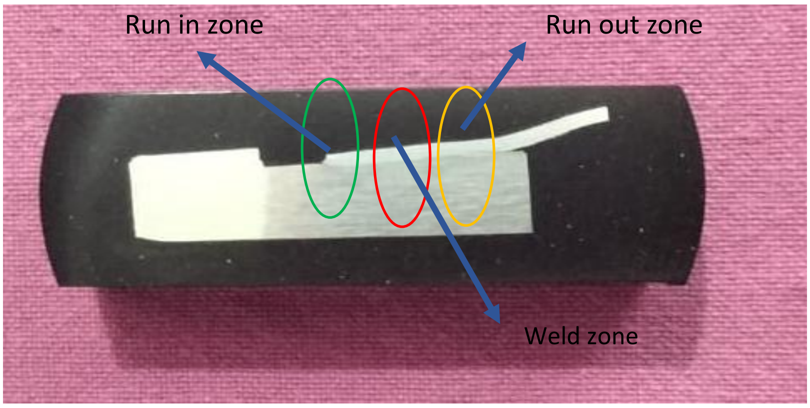

Fig. 16. SEM Pictures of 6 specimens

EDS results [Fig 15(a,b,c)] reveal that there is not much of a difference between the Flyer and Target metals after weld and hence there exists very little variation in Hardness of the base metals. Line scanning results taken right through the weld specimen as in Fig 16 have shown that the percentage of Aluminium at the interface is low in comparison with the base metals and has dilution of Mg and Si elements into the interface. Presence of Mg and Si promote formation of Mg2Si precipitates which increases the hardness of the interface. Sample M3 has Mg and Si in good percentage at the interface with considerable lower percentage of Al as shown in Fig 16 the highest hardness of all samples is due to this reason. The elemental mapping Fig 17 reveals presence of and Mg and Si at the interface of Sample M3 which confirms the reason of high hardness. However, the size of the precipitate will matter for increase in strength, if the size of precipitate is larger it will not allow strain hardening and hence a decreased hardness can be felt at the interface as in the case of Sample M5 [Fig.13(o)].

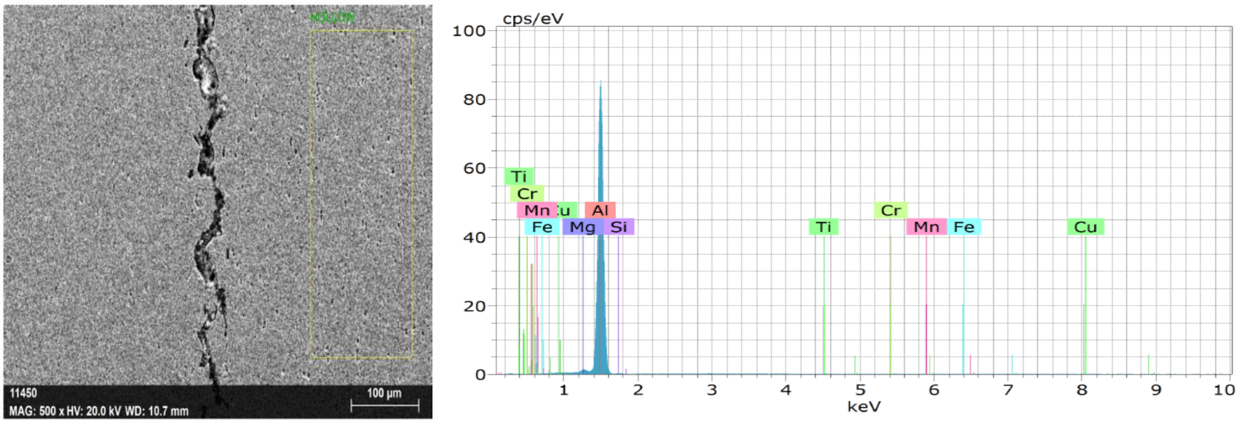

(a) FLYER METAL --Al 6061 T6

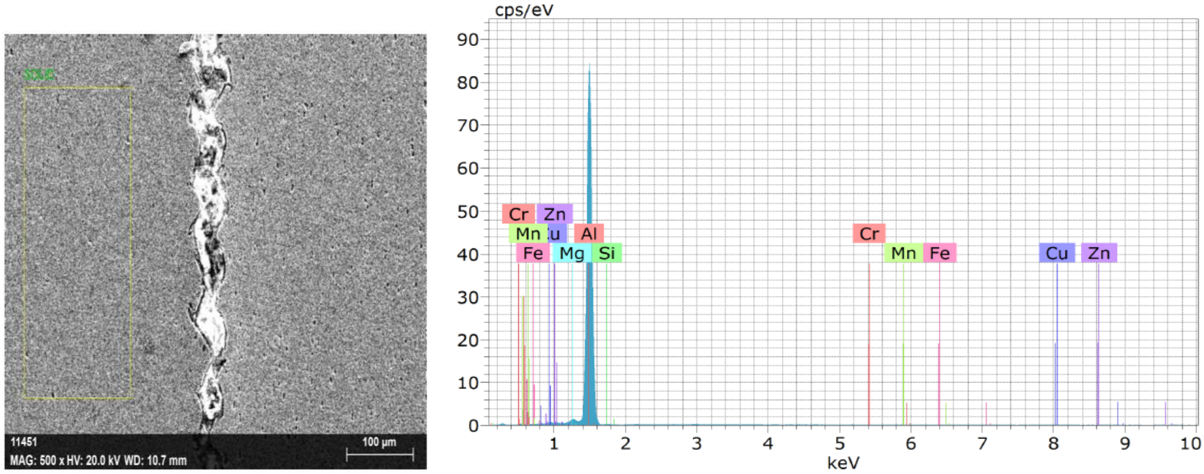

(b) **TARGET METAL-Al 6061 T6**

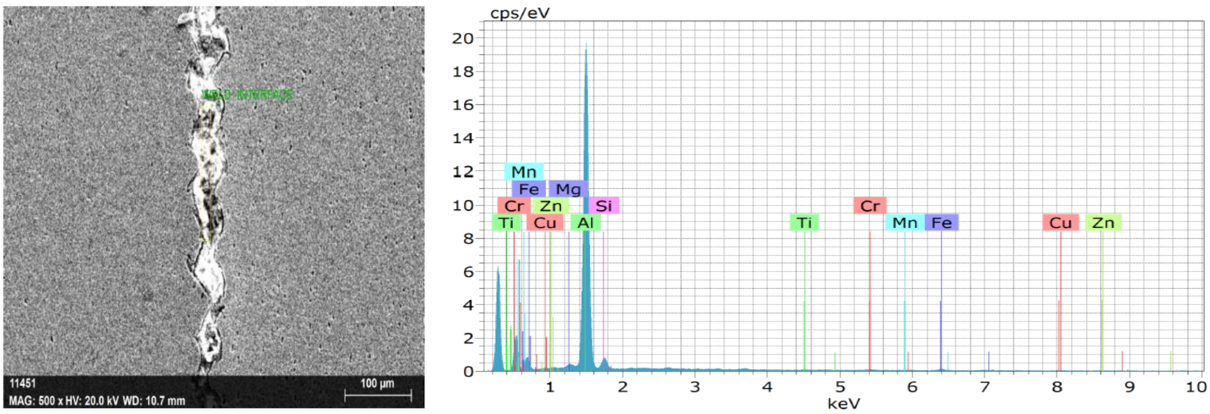

(c) **WELD INTERFACE**

Fig. 17. SEM Pictures of 6 specimens

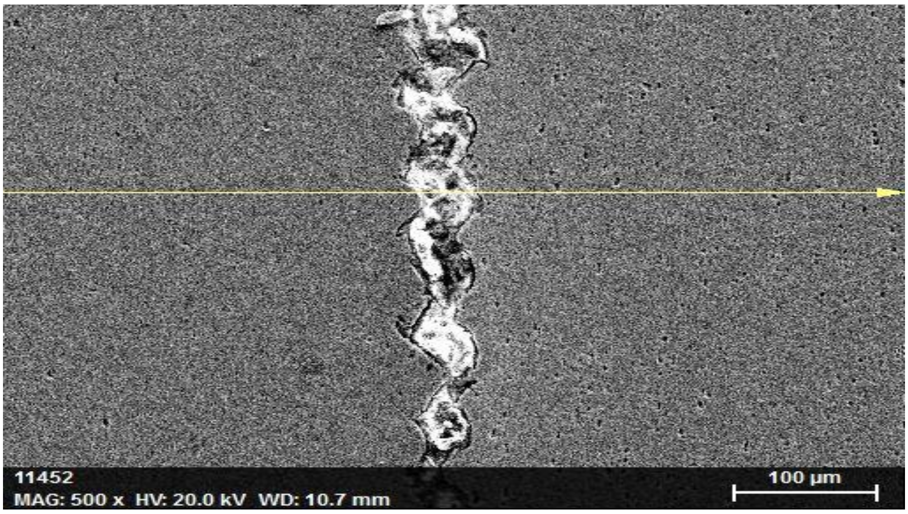

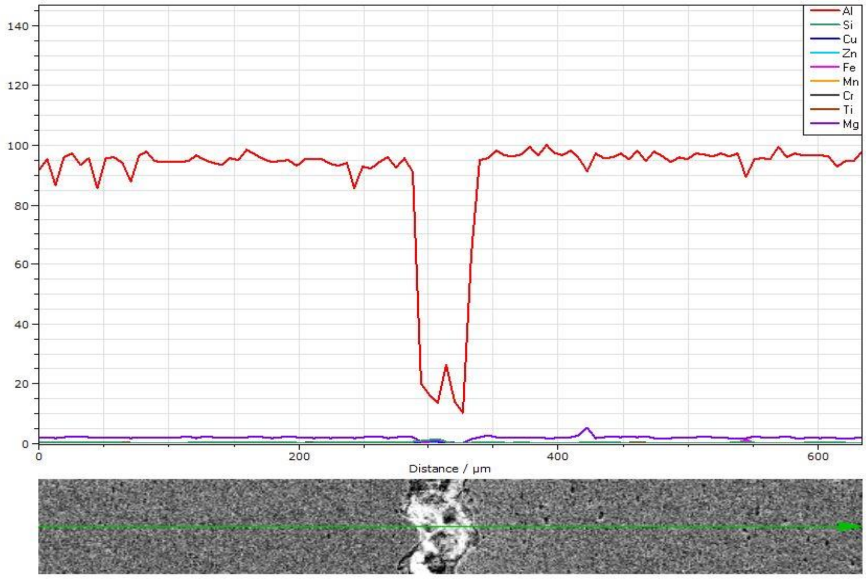

Fig. 18. Line Scanning of sample M3

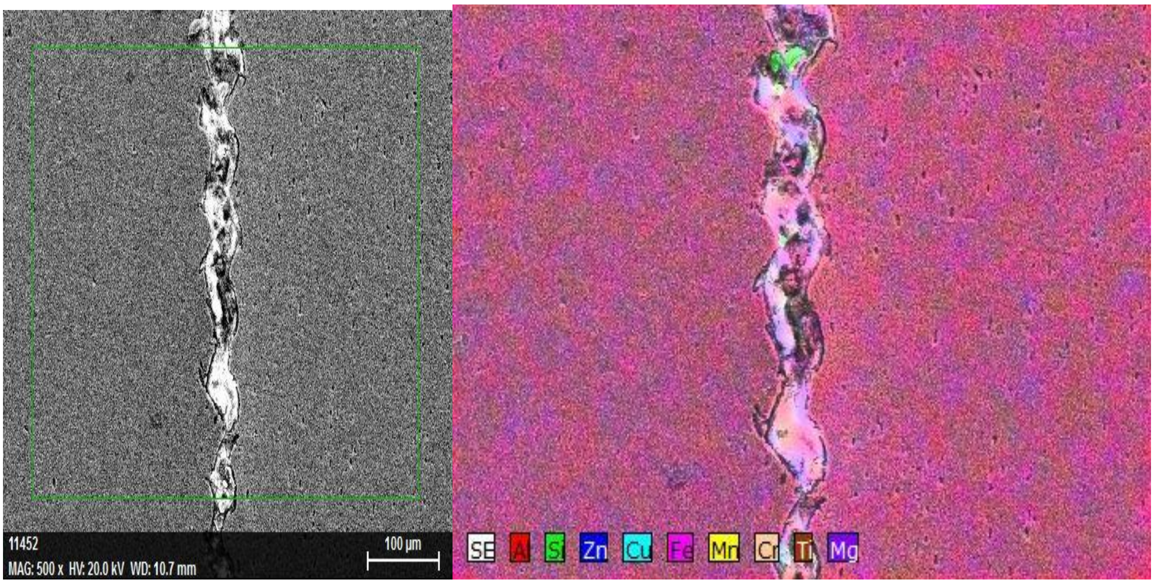

Fig. 19. Elemental Mapping of sample M3

6. Conclusions

In this investigation, similar Aluminium alloys AA 6061 T6 tube–rod were successfully joined using MPW technique in lap configuration and the following conclusions were made.

1. The tensile shear strength of the welded specimens was determined and the optimized value of the Tensile Shear Fracture Load (TSFL) has been identified as 303 MPa for the process parameters Discharge Voltage of 12 kV, Stand-off distance 1.75mm and Overlap length 8 mm.
2. Failure during the tensile test and the Compression test happened at the weakest of the base metals, the Flyer tube which is an indication of sound bonding between the mating parts.
3. Highest tensile strength was observed for sample M3 and the reason can be attributed to the correct combination of process parameters which resulted in a defined wave pattern of the interface.
4. The lower welding interface strength of sample M5 can be related to the insufficient impact velocity due to low Stand-off distance and high discharge voltage (17.33 kV). Sample M5 also exhibited porous welding interface which is potentially facilitated pores nucleation, coalescence and growth in sequential order within the molten intermediate phase and this is very important contributor of reduced tensile strength and hardness in the interface.
5. Microhardness survey across all the weld specimens revealed that Hardness values at the weld interface exceeded the base metals. The highest hardness was observed as 138 HV at the weld interface of sample M3 which is 1.75 times higher than that of the actual base metal hardness. The lowest hardness at the weld interface was observed as 100 HV of sample M5 which is 1.25 times higher than that of the actual base metal hardness. It is concluded that the higher hardness is due to grain refinement caused by severe plastic deformation.
6. SEM analysis reveal similar pattern of metallurgy in the base metals. At the weld interface three patterns were observed, one defined wavy interface, second is a straight interface and third is a discontinuous wave pattern. Highest tensile strength and hardness were observed in sample M3 with defined wave pattern. Lowest tensile strength and hardness were observed in sample M5 with discontinuous wave pattern. Straight interface wave pattern observed in sample M2 resulted in medium tensile strength and hardness.
7. Line Scanning across the weld specimen and elemental mapping study presented that Aluminium percentage was low at the interface while there was considerable presence of Mg and Si at the interface due to dilution of elements during high speed

collision. Since presence of Mg and Si promote formation of Mg_2Si precipitates, the tensile strength and hardness at the interface were on the higher side. This was precisely why Sample M3 showed high tensile strength and hardness out of all other samples.

8. The TSFL values and the hardness values of all the samples are found to be in good agreement with each other.

References

[1] Furth, H. P., Waniek, R. W.: "Production and use of high transient magnetic fields, part I," Rev. Sci. Instr., (1956), vol. 27, p. 195.

[2] M. Kimchi, H. Shao, W. Cheng, P. Krishnaswamy " Magnetic Pulse Welding Aluminium tubes to Steel bars" Welding in the World volume 48, pages19–22 (2004)

[3] Furth, H. P., Levine, M. A., Waniek, R. W.: "Production and use of high transient magnetic fields, part II," Rev. Sci. Instr., (1957), vol. 28, p. 949.

[4] Mishra, Shobhna, Sharma, SurenderKumar,Kumar, Satendra,Sagar, Karuna, Meena, Manraj, Shyam, Anurag "40kJ Magnetic PulseWelding System for Expansion Welding of Aluminium 6061 Tube" Journal of Materials Processing Technology. http://dx.doi.org/10.1016/j.jmatprotec.2016.09.020

[5] R. M. Mirandaa, B. Tomás a, T. G. Santosa, N. Fernandes b "Magnetic pulse welding on the cutting edge of industrial applications" Soldag. Insp. São Paulo, Vol. 19, Nº. 01, p.069-081, Jan/Mar 2014 69

[6] Koen Faes, Irene Kwee and Wim De Waele," Electromagnetic Pulse Welding of Tubular Products: Influence of Process Parameters and Workpiece Geometry on the Joint Characteristics and Investigation of Suitable Support Systems", Metals- MDPI/01st May 2019.

[7] R.N. Raoelisona, N. Buirona, M. Rachika, D. Haye b, G. Franzc, M. Habakc, "Study of the elaboration of a practical weldability window in magnetic pulse welding", Elsevier-Journal of Material Processing Technology/4 March 2013.

[8] Pampa Gosh, Suman Patra, Soumya Chatterjee, Mahadev Shome "Microstructural Evaluation of Magnetic Pulse Welded Plain Carbon Steel Sheets" Journal of Materials Processing Technology/4 November 2017

[9] Haiping Yu, Zhidan Xu, Zhisong Fan, Zhixue Zhao, Chunfeng Li "Mechanical property and microstructure of aluminum alloy-steel tubes joint by Magnetic pulse welding" Elsevier-Materials Science & Engineering A/ 10 November 2012.

[10] Joerg Bellmann, Joern Lueg-Althoff, Sebastian Schulze,Soeren Gies, Eckhard Beyer, and A. Erman Tekkaya "Parameter Identification for Magnetic Pulse Welding Applications" Key Engineering Materials ,ISSN: 1662-9795, Vol. 767, pp 431-438, doi:10.4028/www.scientific.net/KEM.767.431 © 2018 Trans Tech Publications, Switzerland

[11] Ben-Artzy, A. Stern, N. Frage, V. Shribman, O. Sadot "Wave formation mechanism in Magnetic Pulse Welding" International Journal of Impact Engineering 37 (2010) 397–404

[12] Yuan Zhang, Sudarsanam Suresh Babu & Glenn S. Daehn " Interfacial ultrafine-grained structures on aluminum alloy 6061 joint and copper alloy 110 joint fabricated by magnetic pulse welding" Springer, Journal of Material Science (2010) 45:4645–4651 DOI 10.1007/s10853-010-4676-0.

[13] Sapanathan T, Raoelison R, Buiron N, Rachik M. In situ metallic porous structure formation due to ultra high heating and cooling rates during an electromagnetic pulse welding. Scr Mater 2017; 128:10–3.

[14] Marya M, Marya S. Interfacial microstructures and temperatures in aluminium–copper electromagnetic pulse welds. Sci Technol Weld Join 2004; 9: 541–7.